Modulating Unimolecular Charge Transfer by Exciting Bridge Vibrations

ARTICLE *in* JOURNAL OF THE AMERICAN CHEMICAL SOCIETY · NOVEMBER 2009

Impact Factor: 12.11 · DOI: 10.1021/ja907041t · Source: PubMed

8 AUTHORS, INCLUDING:

Zhiwei Lin
Northwestern University
8 PUBLICATIONS **125** CITATIONS
SEE PROFILE

Dequan Xiao
University of New Haven
40 PUBLICATIONS **506** CITATIONS
SEE PROFILE

Spiros S. Skourtis
University of Cyprus
57 PUBLICATIONS **1,433** CITATIONS
SEE PROFILE

J|A|C|S COMMUNICATIONS

Published on Web 11/24/2009

Modulating Unimolecular Charge Transfer by Exciting Bridge Vibrations

Zhiwei Lin,[†] Candace M. Lawrence,[§] Dequan Xiao,[‡] Victor V. Kireev,[†] Spiros S. Skourtis,[||] Jonathan L. Sessler,[§] David N. Beratan,[‡] and Igor V. Rubtsov*,[†]

Department of Chemistry, Tulane University, New Orleans, Louisiana 70118, Departments of Chemistry and Biochemistry, Duke University, Durham, North Carolina 27708, Department of Chemistry and Biochemistry, University of Texas at Austin, Austin, Texas, 78712, and Department of Physics, University of Cyprus, Nicosia 1678, Cyprus

Received August 19, 2009; E-mail: irubtsov@tulane.edu

Nonadiabatic electron transfer (ET) measures the rate of electron tunneling, often facilitated by intervening covalent and nonbonded interactions.[1−4] Bridge structure therefore influences the ET kinetics, and bridge thermal fluctuations are predicted to modulate the tunneling propensity.[4,5] Structure defines the coupling pathways, and thermal fluctuations enable the system to find configurations that enhance the interaction strength.[6] An open and crucial question is whether or not bridge motion can be manipulated (driven) by an external field to control pathway interactions and ET kinetics. Here, we show that mid-IR driving of bridge vibrations produces ET kinetic slowing of a photoinduced charge separation reaction.

Recent theoretical analysis indicates that ET kinetics can be changed by controlling the coherence of inelastic tunneling pathway interferences in a molecular analogue of the double-slit experiment.[1−4,7] In systems with two interfering ET pathways, the excitation of a pathway-specific bridge vibration, which may induce electron-vibration energy exchange, labels the ET pathway and therefore modifies pathway interferences.[1−4,7] Affecting ET rates using mid-IR radiation[3] is generally attractive because ultrashort laser pulses offer subpicosecond perturbation, and radiation in the mid-IR is chemically innocent. In addition to inelastic tunneling, excitation of bridge vibrations can perturb elastic-tunneling kinetics. The donor−acceptor (DA) coupling may be modulated by exciting a bridge vibrational mode without electron−phonon energy exchange. Related ideas for the control of currents in molecular wires are being addressed in the context of molecular electronics and inelastic-tunneling spectroscopy.[8]

Here, we report the first real-time observation of ET rate modulation by mid-IR excitation in a donor-bridge-acceptor (DBA) ensemble.[9] This ensemble consists of an anthracene-derived acceptor linked to a dimethylaniline-containing donor by guanosine−cytidine (GC) hydrogen bonding (Figure 1A). The ET is probed in a 3-pulse experiment, performed with a sequence of UV, mid-IR, and visible pulses (Figure 1B), each of ca. 100 fs duration. The first pulse at 400 nm creates the acceptor-localized electronic excited state (ES) that then "captures" an electron from the donor with an ET rate constant, k_{CS}, of ca. (30 ps)$^{-1}$.[9] After a small time delay, τ, the second pulse centered at 1670 cm^{-1} (and ∼120 cm^{-1} in width) is applied, targeting vibrational modes in DBA labeled in Figure 1A. The third pulse in the visible spectral region probes the sample absorbance as a function of the probe's delay time, T (Figure 1B).

The absorbance changes in the 3-pulse measurements were calculated using the equation $\Delta\text{abs} = D_{IR} - D = \log(I/I_{IR})$, where D_{IR} and D are the optical densities and I_{IR} and I are the probe signals with the IR pump on and off, respectively. Since the mid-IR pulses were chopped at half of the laser repetition rate, and the two consecutively recorded spectra were processed to obtain Δabs, the 3-pulse measurements are sensitive exclusively to changes in the sample induced by vibrational excitation, rather than by the ET process itself.

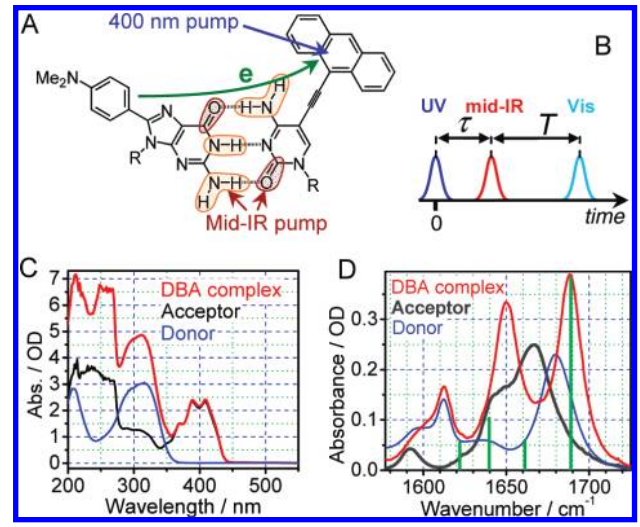

Figure 1. (A) Structure of the DBA complex where R = 2′,3′,5′-tri-*O*-(*tert*-butyldimethylsilyl)ribofuranosidyl. The groups participating most strongly in vibrational modes in the 1630−1700 cm^{-1} range are highlighted. (B) Pulse sequence used in the 3-pulse experiments. Linear UV−vis (C) and mid-IR (D) absorption spectra of the donor and acceptor samples in dichloromethane, both at 20 mM, and their 1:1 (v:v) mixture (DBA) multiplied by a factor of 2. Four DFT-computed vibrational transitions of DBA are shown with green bars. Note that the DFT computed frequencies were scaled down with a factor of 0.948.

The measurements were performed in an all-Teflon flow cell with an optical path length of 130 μm at 23.5 ± 0.3 °C in a nitrogen atmosphere. To minimize the amount of unbound acceptor in the sample ($K_{assoc} = 3.8 \times 10^4$ M^{-1}),[9] all time-resolved measurements were performed in mixtures with a 5-fold molar excess of the donor (75 mM) over the acceptor (15 mM).

Figure 1C shows the UV−vis absorption spectrum of the donor, acceptor, and DBA samples recorded at the same molar concentration. At wavelengths above 280 nm, the spectrum of DBA is the sum of the spectra of the components, indicating weak interaction of the electronic states of the donor and acceptor units. In contrast, the IR spectrum of DBA is not the simple sum of contributions from the two component parts (Figure 1D), clearly demonstrating GC association.

UV-pump/vis-probe spectroscopy was used to measure the transient spectra of the excited and charge separated states of DBA and of the acceptor. The transient spectra of the excited state (ES) and of the charge-separated state (CS) for DBA, measured at a 3

[†] Tulane University.
[§] University of Texas at Austin.
[‡] Duke University.
[||] University of Cyprus.

10.1021/ja907041t

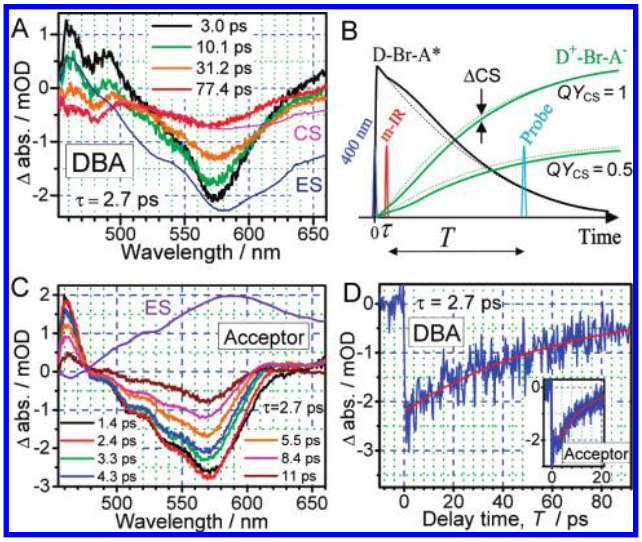

Figure 2. 3-Pulse transient spectra for DBA (A) and the acceptor-only sample (C), measured at $\tau = 2.7$ ps, and different delays, T, indicated. For the acceptor sample (C) the vibronic coupling is the only source of the signal. In contrast, DBA transients have another contribution that can be seen most clearly at later delays, where the transient spectrum matches that of the charge-separated state (CS). To emphasize the similarity, the excited (ES) and charge-separated (CS) state spectra were multiplied by −0.02 (DBA) and 0.01 (acceptor). (B) Simulated kinetic traces illustrating the main expectations in the 3-pulse experiments (see text). (D) 3-Pulse transient kinetics for DBA and for the acceptor (inset) measured at 578.8 and 563.6 nm, respectively. Exponential fits are shown in red. The CS population difference ΔCS is related to Δ abs(λ) by Δ abs(λ) = $\epsilon(\lambda)\, l\, \Delta$CS.

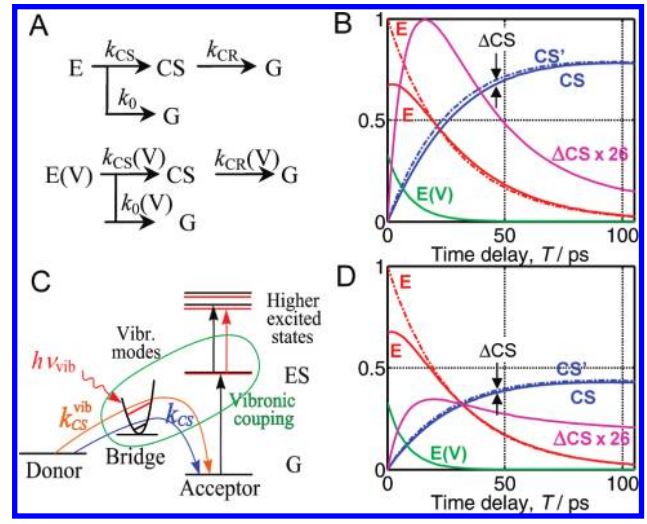

Figure 3. (A) Kinetic scheme used to model the data. (B, D) Populations of the excited and CS states computed for two initial conditions {E, E(V), CS} = {1, 0, 0} (dashed lines) and {0.67, 0.33, 0} (solid lines), which correspond to the cases without and with vibrational excitation, respectively. The quantum yield of CS was 0.9 (B) and 0.5 (D). The fraction of the vibrationally excited DBA molecules (33%) were calculated based on the IR pulse energy (1 μJ), beam size in the sample (150 μm), and the spectral width of the IR pulses (120 cm^{-1}). The difference in the amount of CS states formed without and with vibrational excitation, ΔCS = CS − CS′, scaled by a factor of 26, is shown with magenta. The following parameters were used for the modeling: $k_{CS} + k_0 = (28\ \text{ps})^{-1}$, $k_C = (10.6\ \text{ps})^{-1}$, $k_0 = k_0(V)$, $k_{CR} = k_{CR}(V) = (700\ \text{ps})^{-1}$, $k_{CS}(V) = (90\ \text{ps})^{-1}$. (C) Schematics describing the vibronic coupling effect and the effect of modulation of the CS rate with IR.

and 77.4 ps probe delay, respectively (Figure 2A), were found to be in good agreement with the previous data.[9]

In the 3-pulse measurements, the mid-IR pulses were targeting two strong absorptions of DBA at 1650 and 1689 cm^{-1} (Figure 1D). DFT calculations and normal-mode analysis[10] lead us to assign the peak at 1689 cm^{-1} to an asymmetric stretch of the two carbonyl groups. Note that the DFT computed frequencies were normalized to the absorption peak at 1689 cm^{-1} by scaling down by a factor of 0.948. The peak at 1650 cm^{-1} has several contributions, including a relatively weak symmetric stretch of the carbonyl groups (computed at 1659 cm^{-1}) and in-plane bending modes of the two NH_2 groups (computed at 1640 and 1623 cm^{-1}, Figure 1C, green bars). The CO symmetric stretching mode is too weak to explain the absorbance at 1650 cm^{-1}; in fact, the peak is dominated by NH_2 in-plane bending modes. It is important to appreciate that all vibrational modes with frequencies between 1630 and 1700 cm^{-1} are ascribed to groups in the G−C linkage.

Figure 2A shows the 3-pulse transient spectra for DBA measured at time delays T. Interestingly, the largest transients are observed at small time delays, T. To illustrate the main expectations in the 3-pulse experiment, we computed the kinetic traces for the concentration of the CS state (Figure 2B) formed in the presence of IR excitation (solid green line) and in the absence of IR excitation (dotted green line). Three points are important to note from this modeling. First, the maximum difference between the amount of CS states with and without vibrational excitation (ΔCS), measured in the 3-pulse measurement, occurs at a time delay after the IR pulse (not at $T = 0$). This reflects the fact that time is required to accumulate a different amount of the reaction product as a consequence of IR excitation. Second, at larger time delays T, the difference (ΔCS) diminishes as time progresses (as the charge-separation reaction proceeds to completion). Third, the value of ΔCS observed after completion of the charge-separation reaction depends strongly on the quantum yield of charge separation (QY_{CS}). For example, if $QY_{CS} = 1$ (dark green lines), ΔCS approaches zero when the reaction reaches completion. Most importantly, the transient spectrum at larger probe delays (at which point the vibrationally excited modes have had a chance to cool) should match that of the CS state. In contrast, spectra recorded at small time delays may contain contributions associated with the presence of vibrational excitation (vibronic coupling).

The 3-pulse spectra at small probe delays for DBA (Figure 2A) and for the acceptor (Figure 2C) are dominated by a component that grows within the instrumental response of the experiment (Figure 2D). The transients at small time delays in DBA are derived from coupling of the acceptor-localized electronic excited state with the vibrational modes of the bridge, i.e., vibronic coupling (Figure 3C). A similar transient effect is found in the acceptor-only sample (Figure 2C), confirming the assignment. There are significant differences in the transient spectra of DBA compared to those in the acceptor: the transients of the acceptor decay rapidly (10.6 ps, Figure 2D, inset) and show no spectral changes with time. In contrast, the transient decay is slow in DBA, giving a decay time of 64 ps if fitted with a single-exponential function (Figure 2D), and the spectral shape changes with time (Figure 2A).

Sizable vibronic coupling, seen in both DBA and the acceptor samples, suggests that there is a significant spatial overlap of the acceptor-based excited state and the vibrational modes of the bridge, indicating that the acceptor-based excited state extends to the pyrimidine ring. The decay time of 10.6 ps for the acceptor is assigned to the cooling time of high-frequency modes;[11] vibrational cooling of those modes in DBA is expected to be even faster. Yet, a much longer decay time is observed in DBA (Figure 2D), suggesting that the ET rate is changed by the IR excitation. Indeed, the transients, recorded at larger delay times (77.4 ps), match the spectrum of the CS state. This observation supports the conclusion that a different amount of the CS state accumulates when DBA is

subject to vibrational excitation. The 3-pulse transient spectrum (Δabs) averaged over T of 75−80 ps has an amplitude that is 1.8% of that observed for the CS spectrum (2-pulse UV/vis) measured under the same conditions. The negative sign of the transient spectra indicates that less CS state was produced in the presence of the IR excitation. Note that the observed modulation of the CS yield is not associated with a trivial temperature increase caused by vibrational relaxation of the initially excited modes; preliminary data show that the rate of CS increases at higher temperatures. This temperature effect is obviously different from what is observed under the conditions of vibrational excitation.

A simple kinetic scheme was used to model the results (Figure 3A). E, CS, and G denote the excited, charge-separated, and ground electronic states, respectively; V indicates the presence of high-frequency vibrational excitation of the bridging species. While the decrease of the CS yield can be explained by either a reduction of the CS rate (k_{CS}) and/or an increase in the rate of (mostly) nonradiative decay (k_0), we assume that k_{CS} is affected by vibrational excitation. The modeling showed that the shape of the ΔCS transient kinetics, which is a difference in the amount of the CS state accumulated with and without IR excitation, is very sensitive to the quantum yield of charge separation ($QY_{CS} = k_{CS}/(k_{CS}+k_0)$, Figure 3B,D); the slope of the kinetic traces at larger probe delays ($T > 60$ ps) used to estimate the QY_{CS} resulted in a value of 0.7 ± 0.2. Interestingly, the value of k_{CS}(V) obtained from the modeling is found to vary moderately as a function of QY_{CS}, giving a k_{CS}(V) of $(70-107\text{ ps})^{-1}$ for a quantum yield ranging from 0.5 to 0.9. The cooling time for the modes affecting the CS reaction (k_C) was taken at 10.6 ps, which is the cooling time of high-frequency modes measured for the acceptor. We assume that there are several vibrational modes in DBA that are either excited directly with IR or populated via vibrational relaxation and that these modes can influence the rate of CS. The cooling time strongly affects the value of k_{CS}(V) obtained from the modeling; the actual "action" time for excited modes may differ from the cooling time observed for high-frequency modes (e.g., if lower frequency modes with substantially longer cooling times affect the CS rate). Computed kinetics for the components in the system are shown in Figure 3B and 3D, where the CS quantum yield was taken as 0.9 and 0.5, respectively, while k_{CS}(V) was taken as $(90\text{ ps})^{-1}$, the same for both cases.

Several mechanisms can be proposed to account for the observed decrease of the CS yield upon IR excitation. One mechanism includes a dynamic loosening of the H-bonds by high-frequency vibrational excitation. For example, the H-atom displacement of the NH_2 of guanosine involved with the in-plane bending motion (1622 cm^{-1}) only elongates the H-bond to the carbonyl oxygen of cytidine; it never shortens it. The amplitude of the normal mode at 1622 cm^{-1} (see Supporting Information) was found to be +0.022 Å. Such an IR excitation-induced elongation is expected to affect the H-bond strength and to reduce the DA coupling matrix element that determines the ET rate.[7]

While the lifetime of the excited bending modes is expected to be ca. 1 ps,[12] other modes with lower frequencies will be populated via vibrational relaxation. There are ~10 other modes in DBA that will drive asymmetric H-bond length changes, allowing dynamical modulation of the donor−acceptor coupling. If these changes are fast on the ET time scale, the mean squared DA coupling will enter the ET rate constant.[4] Another mechanism that could reduce the DA coupling matrix element is a dynamic reduction of the guanine and/or cytosine ring planarity, as deformation modes are excited by vibrational relaxation. Indeed, nucleic acid intramolecular distortions were indicated as controlling electronic coupling fluctuations in DNA and PNA ET.[13] The planarity of the bridge hydrogen-bonded pair is expected to influence the DA coupling and the CS rate significantly.[7,14,15] Modulating the planarity of the G and C rings may also enhance the nonradiative relaxation of the excited state to the ground state, reducing the quantum yield of the CS reaction.[15] While the Watson−Crick structure is the dominant one, the presence of other tautomers in quantities up to 2% has been predicted, most notably the imino-enol double hydrogen atom transfer structure.[15,16] The influence of IR on the tautomer distribution in the GC complex may affect the ET rate. It is also possible that inelastic ET channels may contribute to the observed effect.[1,3]

In summary, we have demonstrated, for the first time, that DA charge transfer can be modulated by direct vibrational excitation of bridging modes. Dynamic modulation of the effective DA coupling, by partial disruption of the bridging H-bonds and/or by distortion of the planarity of the bridging π-electron system, is proposed to explain the effect. Several approaches can be envisioned to enhance the effect of modulation, including the use of DA pairs with higher symmetry or those with a better match between the lifetimes of the vibrational modes and the ET time scale. Ultimately, such improvements could lead to the development of new molecule-based charge separating devices, including molecular switches, wherein IR irradiation is used to control the underlying ET kinetics.

Acknowledgment. We thank the NSF (CHE-0718043 to D.N.B. and I.V.R., CHE-074971 to J.L.S.) and the Robert A. Welch Foundation (F-1018) to J.L.S. for support of this research.

Supporting Information Available: Complete ref 10, computational details, and extended FTIR spectrum. This material is available free of charge via the Internet at http://pubs.acs.org.

References

(1) Skourtis, S. S.; Waldeck, D. H.; Beratan, D. N. *J. Phys. Chem. B* **2004**, *108*, 15511–15518.
(2) Newton, M. D. *Int. J. Quantum Chem.* **2000**, *77*, 255–263. Gray, H. B.; Winkler, J. R. *Q. Rev. Biophys.* **2003**, *36*, 341–372. Medvedev, E. S.; Stuchebrukhov, A. A. *J. Chem. Phys.* **1997**, *107*, 3821–3831.
(3) Xiao, D.; Skourtis, S. S.; Rubtsov, I. V.; Beratan, D. N. *Nano Lett.* **2009**, *9*, 1818–1823.
(4) Beratan, D. N.; Skourtis, S. S.; Balabin, I. A.; Balaeff, A.; Keinan, S.; Venkatramani, R.; Xiao, D. *Acc. Chem. Res.* **2009**, *42*, 1669–1678.
(5) Balabin, I. A.; Beratan, D. N.; Skourtis, S. S. *Phys. Rev. Lett.* **2008**, *101*, 158102/158102-1–158102-4.
(6) Skourtis, S. S.; Lin, J.; Beratan, D. N. In *Modern methods for theoretical physical chemistry of biopolymers*; Starikov, E. B., Lewis, J. P., Tanaka, S., Eds.; Elsevier: Boston, MA, 2006.
(7) Skourtis, S. S.; Beratan, D. N. *Adv. Chem. Phys.* **1999**, *106*, 377–452.
(8) Kohler, S.; Lehmann, J.; Hänggi, P. *Phys. Rep.* **2005**, *406*, 379–443. Maddox, J. B.; Harbola, U.; Liu, N.; Silien, C.; Ho, W.; Bazan, G. C.; Mukamel, S. *J. Phys. Chem. A* **2006**, *110*, 6329–6338. Troisi, A.; Beebe, J. M.; Picraux, L. B.; van Zee, R. D.; Stewart, D. R.; Ratner, M. A.; Kushmerick, J. G. *Proc. Natl. Acad. Sci. U.S.A.* **2007**, *104*, 14255–14259.
(9) Sessler, J. L.; Sathiosatham, M.; Brown, C. T.; Rhodes, T. A.; Wiederrecht, G. *J. Am. Chem. Soc.* **2001**, *123*, 3655–3660.
(10) Frisch, M. J. et al. *Gaussian 03*, revision D.02; Gaussian, Inc.; Wallingford, CT, 2004.
(11) Naraharisetty, S. G.; Kasyanenko, V. M.; Rubtsov, I. V. *J. Chem. Phys.* **2008**, *128*, 104502–104507. Seong, N.-H.; Fang, Y.; Dlott, D. D. *J. Phys. Chem. A* **2009**, *113*, 1445–1452.
(12) Rubtsov, I. V. *Acc. Chem. Res.* **2009**, *42*, 1385–1394.
(13) Hatcher, E.; Balaeff, A.; Keinan, S.; Venkatramani, R.; Beratan, D. N. *J. Am. Chem. Soc.* **2008**, *130*, 11752–11761.
(14) Skourtis, S. S.; Onuchic, J. N.; Beratan, D. N. *Inorg. Chim. Acta* **1996**, *243*, 167–175. Zeng, Y.; Zimmt, M. B. *J. Am. Chem. Soc.* **1991**, *113*, 5107–5109. Rubtsov, I. V.; Redmore, N. P.; Hochstrasser, R. M.; Therien, M. J. *J. Am. Chem. Soc.* **2004**, *126*, 2684–2685.
(15) Sobolewski, A. L.; Domcke, W. *Phys. Chem. Chem. Phys.* **2004**, *6*, 2763–2771.
(16) Villani, G. *Chem. Phys.* **2006**, *324*, 438–446.

JA907041T